

# Comprehensive Two-Point Analyses of Weak Gravitational Lensing Surveys

Gary M. Bernstein

*Dept. of Physics and Astronomy, University of Pennsylvania, Philadelphia, PA 19104*

`garyb@physics.upenn.edu`

## ABSTRACT

We present a framework for analyzing weak gravitational lensing survey data, including lensing and source-density observables, plus spectroscopic redshift calibration data. All two-point observables are predicted in terms of parameters of a perturbed Robertson-Walker metric, making the framework independent of the models for gravity, dark energy, or galaxy properties. For Gaussian fluctuations the 2-point model determines the survey likelihood function and allows Fisher-matrix forecasting. The framework includes nuisance terms for the major systematic errors: shear measurement errors, magnification bias and redshift calibration errors, intrinsic galaxy alignments, and inaccurate theoretical predictions. We propose flexible parameterizations of the many nuisance parameters related to galaxy bias and intrinsic alignment. For the first time we can integrate many different observables and systematic errors into a single analysis. As a first application of this framework, we demonstrate that: uncertainties in power-spectrum theory cause very minor degradation to cosmological information content; nearly all useful information (excepting baryon oscillations) is extracted with  $\approx 3$  bins per decade of angular scale; and the rate at which galaxy bias varies with redshift substantially influences the strength of cosmological inference. The framework will permit careful study of the interplay between numerous observables, systematic errors, and spectroscopic calibration data for large weak-lensing surveys.

*Subject headings:* gravitational lensing; cosmological parameters; relativity

## 1. Introduction

Weak gravitational lensing of background sources can produce exceptionally strong constraints on cosmological parameters and tests of General Relativity. Initial analyses considered the 2-point correlation function (or, equivalently, power spectrum) of the shear pattern induced on a single population of background galaxies (Miralda-Escudé 1991; Kaiser 1992; Blandford et al. 1991). A wealth of new statistics, however, have been suggested as more powerful means to extract information from weak lensing (WL): cross-power spectra of multiple source populations with distinct

redshift distributions (a.k.a. “tomography”) (Hu 1999); the correlation of shear with foreground galaxy clusters (Jain & Taylor 2003), or more generally the cross-correlation of lensing shear with the galaxy distribution (Bernstein & Jain 2004; Zhang, Hui, & Stebbins 2003); joint analyses of density-density, density-shear, and shear-shear correlations in an imaging survey (Hu & Jain 2004); cross-correlation of magnification as well as shear (Jain 2002); use of the CMB (Hu & Okamoto 2002; Hirata & Seljak 2003) or recombination-era 21 cm signals (Metcalf & White 2007; Pen 2004; Zahn & Zaldarriaga 2006) as source planes; cross-correlation of source density or shear with a distinct spectroscopic galaxy survey population (Newman 2008; Schneider et al. 2006); and the use of 3-point statistics (Takada & Jain 2004) or statistics such as peak counts (Hennawi & Spergel 2005; Wang, Khoury & Haiman 2004; Marian & Bernstein 2006) to move beyond 2-point information. Each of these potential innovations has been individually analyzed and shown to improve cosmological constraints. The first goal of this paper is to consider the *simultaneous* use of all of these observable statistics: can we forecast the cosmological information that they will yield collectively in future surveys? Can we start to develop a framework in which all these signals could be analyzed simultaneously in a real experiment?

In parallel with the increasing variety of proposed WL signals, the community has identified a series of potential astrophysical and instrumental non-idealities in WL data which, if ignored, would lead to substantial systematic errors in the inferred cosmology. These include: finite accuracy in our ability to predict the deflecting mass power spectrum due to nonlinearities (Jain & Seljak 1997) and baryonic physics (Zhan 2006; Jing *et al.* 2006); intrinsic alignments (IA) between galaxy shapes (Croft & Metzler 2000) and between galaxy shapes and the local mass distribution (Hirata & Seljak 2004) that are not induced by lensing; multiplicative “shear calibration” errors in the derivation of lensing shear from galaxy images (Ishak *et al.* 2004; Huterer et al. 2006); additive “spurious shear” due to uncorrected PSF ellipticity or other imaging systematics (Huterer et al. 2006; Amara & Refregier 2007); and errors in the assignment of redshifts to the source populations (Ma, Hu, & Huterer 2006). The impact of these systematic-error sources on cosmological inferences have been analyzed by different means, but a second goal of this paper is to produce a comprehensive forecast that considers the presence of them all simultaneously.

Previous work has shown that these multiple sources of information and systematic in WL surveys can interact in interesting ways. For example, in the presence of tomographic data, many systematics are readily distinguishable from cosmological signals and can hence be diagnosed and corrected internally to a survey; this approach is called *self-calibration* (Huterer et al. 2006). It has also been shown that combining galaxy density and lensing correlations can lead to self-calibration of shear calibration errors (Bernstein & Jain 2004) and the uncertainties in galaxy biasing (Hu & Jain 2004; Zhan 2006). Intrinsic alignments of galaxies can be diagnosed and corrected if tomographic information is available (King & Schneider 2003), however this places substantially greater demands on the precision and accuracy of redshift assignment than would otherwise be needed (Bridle & King 2007). These investigations raise important practical questions: will the self-calibration techniques continue to succeed when we attempt to simultaneously self-calibrate several different systematic

errors? Do cross-correlation techniques reduce uncertainties in redshift distributions to negligible levels, or is it necessary to make a complete spectroscopic redshift survey of some size to measure redshift distributions directly (Ma & Bernstein 2008)? This paper will present a formalism through which all these questions can be answered, but we defer to later papers the application of the framework to these issues.

A third goal of this work is to describe the constraints by WL in a language that is not tied to a specific cosmological model. Most forecasts for WL survey constraints are done within the context of a Universe that has homogeneous dark energy with equation of state  $w = w_0 + w_a(1 - a)$ . Projecting the WL experiment onto this model gives concrete predictions, but obscures what the WL is really measuring. So the analysis framework presented here will be *dark-energy agnostic*, meaning that no specific model is assumed. We will be very explicit about the assumptions made in the analysis and try to keep them to a minimum. In fact a great strength of WL experiments are their ability to test General Relativity itself, so we seek an analysis method that is general enough to incorporate such tests. Similar to the approach of Knox, Song, & Tyson (2006), our analysis results in constraints on the distance and growth functions  $D(z)$  and  $g_\phi(z)$ , without reference to the particular dark-energy or gravity modifications that might cause deviations from  $\Lambda$ CDM.

In the following section we describe a “kitchen-sink” formalism for WL survey observables that allows the incorporation of all suggested 2-point statistics and very general treatments of nearly all proposed systematic errors. In §3 we give a likelihood function and Fisher matrix for an unbiased spectroscopic redshift survey of source galaxies. Then we briefly describe a software implementation of the lensing and spectroscopy likelihood calculations. We describe our model for the evolution of the lensing-potential power spectrum in §5, and §6 we describe generic models used for the nuisance functions required in the lensing-survey analysis. In §7 we use the implementation of these methods to investigate the proper choices for the bin sizes and grid spacings needed to turn the lensing analysis into a tractable finite-dimensional problem. Further application of the framework to survey forecasting will be done in future papers.

An earlier version of this WL analysis formalism was used to generate forecasts for the Dark Energy Task Force (Albrecht et al. 2006), and is described in an appendix to that report.

## 2. The Weak Lensing 2-Point Likelihood

### 2.1. Observables

We make the assumption that *the Universe has only weak scalar perturbations to a homogeneous and isotropic 4-dimensional metric*. In this case the metric can be written in the Newtonian gauge as a perturbed Robertson-Walker metric:

$$ds^2 = (1 + 2\Psi)dt^2 - a^2(t)(1 + 2\Phi) [d\chi^2 + \chi_0^2 S_k^2(\chi/\chi_0)(d\theta^2 + \sin^2\theta d\varphi^2)] \quad (1)$$

We assign all mass and sources in the Universe to a series of narrow spherical shells centered at redshifts  $a_i = (1 + z_i)^{-1}$  for  $i \in \{1, \dots, N_z\}$ . There is a comoving angular diameter distance  $D_i$  to each shell, and the comoving radial extent of each shell is  $\Delta\chi_i$ . Note that the Robertson-Walker metric formula for angular-diameter distance is  $D = \chi_0 S_k(\chi/\chi_0)$ , where  $\chi_0$  is the comoving radius of curvature of the Universe. For small values of the curvature  $\omega_k \equiv -k/\chi_0^2$  we have

$$\Delta\chi_i \approx \Delta D(1 - \omega_k D_i^2/2) = \frac{D_{i+1} - D_{i-1}}{2}(1 - \omega_k D_i^2/2). \quad (2)$$

The Robertson-Walker metric also requires  $\Delta\chi_i = \Delta z_i/h(z_i) = \Delta a_i/a_i^2 h(a_i)$ . In this paper the Hubble parameter will be written as  $H(z) = h(z)H_{100}$ ,  $H_{100} = 100 \text{ km s}^{-1} \text{ Mpc}^{-1}$ , and all distances will be in units of  $c/H_{100} = 2998 \text{ Mpc}$ .

We assume that the photon sources in a survey will be divided into a series of *sets*  $\alpha \in \{1, 2, \dots, N_s\}$ . Note the use of latin indices for redshift shells, greek for source sets. We follow Hu & Jain (2004) by assigning each source set up to two observables: first its sky-plane density fluctuations  $g_\alpha(\theta, \varphi)$ , and second a lensing convergence  $\kappa_\alpha(\theta, \varphi)$ . The convergence  $\kappa$  might be inferred from the shear or flexion (Goldberg & Bacon 2005) of galaxies, by a quadratic estimator on the CMB or 21-cm radiation fluctuations, or by any other observable except the source density. The sources can be assigned to sets by photometric or spectroscopic redshift, or even cruder color criteria (Jain et al. 2007), but there could be other criteria such as galaxy type, or perhaps observation by different instruments. We demand only that the criteria for division of the sources be spatially homogeneous, and that the division be invariant under application of gravitational lensing distortion. For notational convenience we assign each set a nominal redshift  $z_\alpha$ , but a set can span a broad redshift range. If the sources are discrete objects such as galaxies, then the mean density on the sky of members of each set are denoted  $n_\alpha$ .

A source in set  $\alpha$  has a probability  $p_{\alpha i}$  of lying on redshift shell  $i$ . The collection of galaxies in set  $\alpha$  on shell  $i$  will be called the *subset*  $\alpha i$ . The survey is assumed to tell us only which *set* any individual galaxy belongs to, but not which *subset*. The  $p_{\alpha i}$  are parameters which must be constrained by the lensing survey data or by additional observations, *e.g.* a spectroscopic redshift survey.

When the lensing sources are drawn from a spectroscopic survey (or when the source is the CMB), then the redshift probability is known *a priori*, and in particular the sets are probably divided by redshift so that  $p_{\alpha i}$  is essentially the identity matrix. The formalism can obviously accommodate the simultaneous analysis of WL samples with varying modes of redshift assignment.

Both the source density fluctuation  $g_\alpha$  and convergence  $\kappa_\alpha$  have a component due to intrinsic fluctuations plus a component due to gravitational lensing. Both are also measured as weighted sums over their respective subsets. We have

$$1 + g_\alpha(\theta, \varphi) = \sum_i p_{\alpha i} [1 + g_{\alpha i}^{\text{int}}(\theta, \varphi)] [1 + q_{\alpha i} \kappa_i^{\text{lens}}(\theta, \varphi)] \quad (3)$$

$$\kappa_\alpha(\theta, \varphi) = \sum_i p_{\alpha i} \left[ \kappa_{\alpha i}^{\text{int}}(\theta, \varphi) + (1 + f_{\alpha i}) \kappa_i^{\text{lens}}(\theta, \varphi) \right]. \quad (4)$$

Here we have assigned each subset a *magnification bias factor*  $q_{\alpha i}$  and a *shear calibration factor*  $f_{\alpha i}$ . In a simple flux-limited selection, the magnification bias factor will be determined by the logarithmic slope of the counts vs flux, and is typically of order unity. The shear calibration factor allows for the possibility that the inferred lensing convergence is mis-measured by some factor  $1 + f_{\alpha i}$  due to multiplicative errors in the lensing methodology, *e.g.* as investigated by Heymans et al. (2006).

In the limit  $g^{\text{int}} \ll 1$  and  $\kappa^{\text{lens}} \ll 1$ , we can drop the second-order term in Equation 3 and write

$$g_\alpha = \sum_i p_{\alpha i} \left[ g_{\alpha i}^{\text{int}} + q_{\alpha i} \kappa_i^{\text{lens}} \right] \quad (5)$$

$$\kappa_\alpha = \sum_i p_{\alpha i} \left[ \kappa_{\alpha i}^{\text{int}} + (1 + f_{\alpha i}) \kappa_i^{\text{lens}} \right]. \quad (6)$$

In this case the equations are linear in all the angular functions  $g$  and  $\kappa$ , so we can decompose them into spherical harmonic coefficient  $g_{\alpha \ell m}$ ,  $\kappa_{i \ell m}^{\text{lens}}$ , etc, and Equations (5) and (6) hold independently for every harmonic  $\ell m$ . We will henceforth assume that the spherical-harmonic decomposition has been executed for all the angular functions  $g$ ,  $\kappa$ , and suppress the  $\ell m$  indices for brevity.

We note that while  $\kappa^{\text{lens}} \ll 1$  is a good approximation over most of the sky,  $g^{\text{int}} \ll 1$  is a poor approximation for thin density slices on smaller angular scales. We will forge ahead nonetheless with the assumption that *lensing magnification simply adds to the intrinsic density fluctuations*, recognizing that a real analysis of data with magnification bias may require inclusion of the nonlinear coupling between spherical harmonics that is induced by magnification bias on highly structured density fields.

The lensing convergence is determined entirely by the metric if we make the assumption that light rays are following its null geodesics. The paths of null geodesics are determined by the *lensing potential*

$$\phi \equiv \frac{1}{2}(\Psi - \Phi). \quad (7)$$

For each of our redshift shells we define a projected lensing potential via

$$\psi_i \equiv 2\nabla_\theta^2 \int_{\Delta\chi} \phi a d\chi, \quad (8)$$

where the derivatives are taken with respect to angles on the sky. We will generally assume that  $\psi$ , like the observables, has been decomposed into spherical harmonics, and we will take the flat-sky approximation.

With the definition (8), and the adoption of the weak-lensing limit and Born approximation, the lensing convergence is

$$\kappa_i^{\text{lens}} = \sum_j A_{ij} \frac{\psi_j}{2a_j D_j}, \quad (9)$$

$$A_{ij} \equiv \begin{cases} \frac{D_{ij}}{D_i} \approx (1 - D_j/D_i)(1 - \omega_k D_i D_j/2) & z_i > z_j, \\ 0 & z_i \leq z_j. \end{cases} \quad (10)$$

$D_{ij}$  is the comoving angular diameter distance to  $z_i$  as viewed from  $z_j$ . In summary, the observables from the survey are, for each spherical harmonic:

$$\begin{aligned} g_\alpha &= \sum_i p_{\alpha i} \left[ q_{\alpha i} \sum_j A_{ij} \frac{\psi_j}{2a_j D_j} + g_{\alpha i}^{\text{int}} \right] \\ \kappa_\alpha &= \sum_i p_{\alpha i} \left[ (1 + f_{\alpha i}) \sum_j A_{ij} \frac{\psi_j}{2a_j D_j} + \kappa_{\alpha i}^{\text{int}} \right]. \end{aligned} \quad (11)$$

We reiterate that these equations depend only upon the assumption of a Robertson-Walker metric with scalar perturbations, plus the approximation that magnification bias and intrinsic density fluctuations are additive.

The equations for the two observables are symmetric under the interchange of  $g \leftrightarrow \kappa$  and  $q \leftrightarrow (1 + f)$ . Since  $q \sim 1 + f$ , the lensing effects are similar. However the intrinsic density fluctuations  $g^{\text{int}}$  are  $\approx 300\times$  stronger than  $\kappa^{\text{int}}$ , breaking the symmetry. Density-field observations are dominated by the intrinsic signal while convergence (shear) observations are dominated by lensing effects.

## 2.2. Degeneracies

Equations (9)–(11) reveal a family of degeneracies present in lensing observations, as described in Bernstein (2006). The transformations

$$\begin{aligned} D_j &\rightarrow D_j(1 + \alpha_0 + \alpha_1 D_j + \alpha_2 D_j^2) \\ \psi_i &\rightarrow \psi_i(1 + \alpha_0 + 2\alpha_1 D_j + 2\alpha_2 D_j^2) \\ \omega_k &\rightarrow \omega_k + 2\alpha_2 \end{aligned} \quad (12)$$

leave the observables unchanged, to first order in  $\{\alpha_0, \alpha_1 D, \alpha_2 D^2, \omega_k D^2\}$ . It will hence be impossible for lensing+density surveys to constrain  $\omega_k$  or any quadratic (in  $D$ ) deviations to  $\ln D$ , unless there are prior constraints on these variables or on  $\psi, g^{\text{int}}$ , or  $\kappa^{\text{int}}$ . Constraint on these three degeneracies is unlikely to arise from models of intrinsic clustering or alignment, since it is unlikely that *a priori* models of the redshift dependence of galaxy bias could reach high precision. We hence expect that these degeneracies are going to be broken by theoretical models of the potential fluctuation power spectrum, or by other distance indicators such as supernovae or BAO.

### 2.3. Limber Approximation

To forecast the constraints on the parameters of this model, we require a likelihood expression for the observables. The two fundamental assumptions we make are:

1. The distributions of the lensing potential, intrinsic galaxy density fluctuations, and intrinsic shape correlations  $\psi_i, g_{\alpha i}^{\text{int}}$ , and  $\kappa_{\alpha i}^{\text{int}}$  are described by a multivariate Gaussian with zero mean.
2. The Limber approximation is valid and there is no correlation between these variables on distinct redshift shells or between different spherical harmonics:

$$\begin{aligned}
 \langle X_{ilm} Y_{j\ell'm'} \rangle &= \delta_{ij} \delta_{\ell\ell'} \delta_{mm'} (D_i^2 \Delta \chi_i)^{-1} P_i^{XY}(\ell/D_i) \\
 \langle X_{ilm} \psi_{j\ell'm'} \rangle &= -2 \delta_{ij} \delta_{\ell\ell'} \delta_{mm'} a_i (\ell/D_i)^2 P_i^{X\phi}(\ell/D_i) \\
 \langle \psi_{ilm} \psi_{j\ell'm'} \rangle &= \delta_{ij} \delta_{\ell\ell'} \delta_{mm'} 4a_i^2 D_i^2 \Delta \chi_i (\ell/D_i)^4 P_i^{\phi\phi}(\ell/D_i)
 \end{aligned} \tag{13}$$

where  $X, Y \in \{g^{\text{int}}, \kappa^{\text{int}}\}$ , and  $P_i^{XY}(k)$  is the 3-d cross-spectrum of variables  $X$  and  $Y$  at epoch  $a_i$ .

The first assumption insures that the likelihood of an observation is fully specified by the expected covariance matrix of the observables. The second assumption implies that this covariance matrix can be expressed in terms of the 3-d cross-power spectra of the lensing potential, subset densities, and subset intrinsic correlations  $\{\phi_i, g_{\alpha i}^{\text{int}}, \kappa_{\alpha i}^{\text{int}}\}$  at each redshift shell.

### 2.4. Biases and Correlations

A typical convention is to express the galaxy density power  $P^{gg}$  as a bias-scaled version of the mass spectrum  $P^m$ , plus a Poisson shot-noise contribution, and then describing the mass-galaxy covariance  $P^{mg}$  with a correlation coefficient:

$$P^{gg} = (b^g)^2 P^m + \frac{1}{\rho} \tag{14}$$

$$P^{mg} = b^g r^g P^m. \tag{15}$$

The comoving volume number density  $\rho$  of the sources determines the shot noise for a Poisson process, but there is no guarantee that the galaxies are distributed in the mass distribution by a Poisson process. Even when the galaxies do not have Poissonian shot noise, we can still usually write the power in this way for some bias parameter  $b$ ; we just might keep in mind that  $r^g > 1$  is formally allowed if the sources are not Poisson-distributed.

Most generally, both the bias and correlation coefficients are different for each source *subset* as well as being functions of comoving wavenumber  $k$ . Each set  $\alpha$  has a nominal redshift  $z_\alpha$ , and each subset has a redshift deviation  $\Delta z_{\alpha i} = z_i - z_\alpha$ . Galaxies with bad photo-z errors could easily

have different bias from those with good photo- $z$ 's; for example, highly-biased early types tend to have better photo- $z$ 's. So our analysis methods should allow for this complication.

We will adopt the bias/correlation notation for the intrinsic galaxy density fluctuations *and* for the intrinsic convergence  $\kappa^{\text{int}}$ , except that we will parameterize the bias and covariance with respect to the lensing potential rather than mass distribution. If  $P_{i\alpha\beta}^{gg}$  is the 3d cross-power between density fluctuations in subsets  $\alpha i$  and  $\beta i$  at wavenumber  $k$ , and we write  $P_i^\phi$  for the lensing-potential 3d power spectrum, then we express:

$$\begin{aligned} P_{i\alpha\beta}^{gg} &= b_{\alpha i}^g b_{\beta i}^g r_{\alpha\beta i}^{gg} \left( \frac{2a_i}{3\omega_m} \right)^2 k^4 P_i^\phi + \frac{\delta_{\alpha\beta}}{\rho_{\alpha i}} \\ P_{i\alpha\beta}^{\kappa\kappa} &= b_{\alpha i}^\kappa b_{\beta i}^\kappa r_{\alpha\beta i}^{\kappa\kappa} \left( \frac{2a_i}{3\omega_m} \right)^2 k^4 P_i^\phi + \frac{\delta_{\alpha\beta} \sigma_\gamma^2}{\rho_{\alpha i}} \\ P_{i\alpha\beta}^{g\kappa} &= b_{\alpha i}^g b_{\beta i}^\kappa r_{\alpha\beta i}^{g\kappa} \left( \frac{2a_i}{3\omega_m} \right)^2 k^4 P_i^\phi \end{aligned} \quad (16)$$

where  $\rho_{\alpha i}$  is a comoving volume density of the galaxy subset in the shell and  $\sigma_\gamma$  is a measure of the shear noise per galaxy. These describe the normal ‘‘shape noise’’ term in the shear power spectrum and the shot noise in the density field. If flexions or other observables are used to infer the convergence, then the shape noise term may have a different form.

And if  $P_{i\alpha}^{g\phi}$  is the cross-power between the density of subset  $i\alpha$  and lensing potential, we express

$$\begin{aligned} P_{i\alpha}^{g\phi} &= -b_{\alpha i}^g r_{\alpha i}^g \frac{2a_i}{3\omega_m} k^2 P_i^\phi \\ P_{i\alpha}^{\kappa\phi} &= -b_{\alpha i}^\kappa r_{\alpha i}^\kappa \frac{2a_i}{3\omega_m} k^2 P_i^\phi. \end{aligned} \quad (17)$$

Note that specifying the bias and correlation  $b^\kappa$  and  $r^\kappa$  of the intrinsic convergence with the lensing potential is equivalent to giving the ‘‘GI’’ and ‘‘II’’ intrinsic-alignment information, in the notation of Hirata & Seljak (2004).

The lensing power  $P^\phi$  is a function of  $z$  and  $k$ . The biases and correlation coefficients  $b_{\alpha i}^\kappa$ ,  $r_{\alpha i}^\kappa$ ,  $b_{\alpha i}^g$ , and  $r_{\alpha i}^g$  are functions of  $k$ , the nominal redshift  $z_\alpha$  of the source set, and  $\Delta z_{\alpha i}$ , the difference between the subset redshift and the nominal set redshift.

Most complicated are the cross-correlation coefficients such as  $r_{\alpha\beta i}^{gg}$ , which are, most generally, functions of  $k$ ,  $z_i$ , and *both* redshift errors  $\Delta z_{\alpha i}$  and  $\Delta z_{\beta i}$ . In order for the covariance matrix of all these fields to be symmetric, we require  $r_{\alpha\alpha i}^{gg} = r_{\alpha\alpha i}^{\kappa\kappa} = 1$  and the symmetry  $r_{\alpha\beta i}^{XY} = r_{\beta\alpha i}^{YX}$ . Otherwise the correlation coefficients are free to vary, subject to the constraint that the overall correlation matrix of the potential and all fluctuations must remain non-negative.

This parameterization of the fluctuations of the potential and the intrinsic fluctuations is completely general—we have not introduced any further assumptions into the model as long as all the  $b$ 's and  $r$ 's and  $P^\phi$ 's are free parameters (non-negative in the last case).

## 2.5. The Two-Point Statistics

Combining the formula for observables (11), the Limber formulae (13), and the bias notation (16), (17), the covariance matrix for the observables  $\{g_\alpha, \kappa_\alpha\}$  at a given multipole can be broken into three submatrices:

$$\begin{aligned}
 C_{\alpha\beta}^{gg} \equiv \langle g_\alpha g_\beta \rangle &= \sum_{ij} p_{\alpha i} p_{\beta j} \left\{ q_{\alpha i} q_{\beta j} \sum_n A_{in} A_{jn} \Delta \chi_n k_n^4 P_n^\phi(k_n) \right. \\
 &+ q_{\alpha i} A_{ij} \frac{2a_j}{3\omega_m} D_j^{-1} b_{\beta j}^g r_{\beta j}^g k_j^4 P^\phi(k_j) \\
 &+ q_{\beta j} A_{ji} \frac{2a_i}{3\omega_m} D_i^{-1} b_{\alpha i}^g r_{\alpha i}^g k_i^4 P^\phi(k_i) \\
 &\left. + \delta_{ij} \left( \frac{2a_i}{3\omega_m} \right)^2 D_i^{-2} \Delta \chi_i^{-1} b_{\alpha i}^g b_{\beta i}^g r_{\alpha\beta i}^{gg} k_i^4 P^\phi(k_i) \right\} + \frac{\delta_{\alpha\beta}}{n_\alpha}
 \end{aligned} \tag{18}$$

$$\begin{aligned}
 C_{\alpha\beta}^{\kappa g} \equiv \langle \kappa_\alpha g_\beta \rangle &= \sum_{ij} p_{\alpha i} p_{\beta j} \left\{ (1 + f_{\alpha i}) q_{\beta j} \sum_n A_{in} A_{jn} \Delta \chi_n k_n^4 P_n^\phi(k_n) \right. \\
 &+ (1 + f_{\alpha i}) A_{ij} \frac{2a_j}{3\omega_m} D_j^{-1} b_{\beta j}^g r_{\beta j}^g k_j^4 P^\phi(k_j) \\
 &+ q_{\beta j} A_{ji} \frac{2a_i}{3\omega_m} D_i^{-1} b_{\alpha i}^\kappa r_{\alpha i}^\kappa k_i^4 P^\phi(k_i) \\
 &\left. + \delta_{ij} \left( \frac{2a_i}{3\omega_m} \right)^2 D_i^{-2} \Delta \chi_i^{-1} b_{\alpha i}^\kappa b_{\beta i}^g r_{\alpha\beta i}^{\kappa g} k_i^4 P^\phi(k_i) \right\} + \frac{\delta_{\alpha\beta}}{n_\alpha}
 \end{aligned} \tag{19}$$

$$\begin{aligned}
 C_{\alpha\beta}^{\kappa\kappa} \equiv \langle \kappa_\alpha \kappa_\beta \rangle &= \sum_{ij} p_{\alpha i} p_{\beta j} \left\{ (1 + f_{\alpha i})(1 + f_{\beta j}) \sum_n A_{in} A_{jn} \Delta \chi_n k_n^4 P_n^\phi(k_n) \right. \\
 &+ (1 + f_{\alpha i}) A_{ij} \frac{2a_j}{3\omega_m} D_j^{-1} b_{\beta j}^\kappa r_{\beta j}^\kappa k_j^4 P^\phi(k_j) \\
 &+ (1 + f_{\beta j}) A_{ji} \frac{2a_i}{3\omega_m} D_i^{-1} b_{\alpha i}^\kappa r_{\alpha i}^\kappa k_i^4 P^\phi(k_i) \\
 &\left. + \delta_{ij} \left( \frac{2a_i}{3\omega_m} \right)^2 D_i^{-2} \Delta \chi_i^{-1} b_{\alpha i}^\kappa b_{\beta i}^\kappa r_{\alpha\beta i}^{\kappa\kappa} k_i^4 P^\phi(k_i) \right\} + \delta_{\alpha\beta} \left( \frac{\sigma_\gamma^2}{n} \right)_\alpha
 \end{aligned} \tag{20}$$

The comoving wavevector is  $k_i = \ell/D_i$ . In each equation, note that only one of the last three terms is non-zero, depending on whether  $j < i$ ,  $j > i$ , or  $j = i$ , respectively. For the shear-shear correlation  $C^{\kappa\kappa}$ , the  $i = j$  term is recognizable as the ‘‘II’’ intrinsic-correlation effect of Hirata & Seljak (2004), while the  $i < j$  and  $j > i$  terms are their ‘‘GI’’ effect.

Note that the last term in the density-shear expression  $C^{\kappa g}$  is an additional intrinsic-correlation term, between the galaxy density and the intrinsic shapes, which is distinct from the covariance between the lensing potential and shear. This galaxy-shear correlation has been constrained in the context of systematic errors to ‘‘galaxy-galaxy’’ lensing, *e.g.* Bernstein & Norberg (2002); Faltenbacher et al. (2007); Hirata et al. (2004).

Examining the density-density correlation  $C^{gg}$  we find the final term has the normal expected form, but the first three terms describe correlations induced by lensing magnification.

Finally we note that the covariance matrix manifests the same symmetries for  $g \leftrightarrow \kappa$  that were discussed at the end of §2.1.

## 2.6. Likelihood and Fisher matrix

Under our Gaussian assumption, the likelihood functions for the observables are independent at each multipole  $\ell m$ . We define a data vector  $\mathbf{d}_{\ell m}$  to be the union of the  $g_\alpha$  and  $\kappa_\alpha$  observables at each multipole, and  $\mathbf{C}_\ell$  to be the covariance matrix derived above. Under our Gaussian assumption, the total likelihood for the survey is

$$-2 \ln L = \sum_{\ell m} [\mathbf{d}_{\ell m}^T \mathbf{C}_\ell^{-1} \mathbf{d}_{\ell m} + \ln |\mathbf{C}_\ell|]. \quad (21)$$

Forecasts of survey performance are made using the Fisher matrix. The usual formula for zero-mean Gaussian distributions applies (Tegmark, Taylor, & Heavens 1997). We reduce the mode sum to a series of  $N_\ell$  bins centered on multipoles  $\ell_i$ , then the Fisher matrix element for parameters  $p$  and  $q$  is

$$F_{pq} = \sum_{i=1}^{N_\ell} \frac{(2\ell_i + 1) \Delta \ell_i f_{\text{sky}}}{2} \text{Tr} \left[ \mathbf{C}_{\ell_i}^{-1} \frac{\partial \mathbf{C}_{\ell_i}}{\partial p} \mathbf{C}_{\ell_i}^{-1} \frac{\partial \mathbf{C}_{\ell_i}}{\partial q} \right]. \quad (22)$$

Examination of Equations (18)–(20) shows that all derivatives of  $\mathbf{C}$  with respect to parameters are very simple. The calculation of the Fisher matrix is reduced to rapid linear algebra, significantly accelerated by exploiting the very sparse nature of most of the derivative matrices.

We have thus succeeded in producing a likelihood function for the most general joint lensing+density survey, for the case of Gaussian likelihoods limited to 2-point statistics. Given a likelihood we can of course form a Fisher matrix for forecasting, or we can execute a maximum-likelihood analysis of real data. Since this likelihood function makes no mention of a particular dark-energy theory, we see that the parameterization chosen here permits a highly flexible analysis. Indeed no theory of gravity or initial conditions of the Universe have been assumed either, just the existence of a Newtonian gauge metric on a RW background cosmology. The lensing-potential power spectrum  $P^\phi(k, z)$  appears as a series of free parameters, as do the bias and correlation coefficients of the galaxy density and intrinsic alignments.

We have variables that describe, in the most general possible fashion, the important systematic errors, excepting additive shear contamination:

1. Uncertainty in power-spectrum theory will be expressed through prior distributions on the  $P_i^\phi$  parameters.
2. Shear calibration errors arises through finite prior uncertainty on the  $f_{\alpha i}$ .

3. Magnification-bias calibration errors arises through finite prior uncertainty on the  $q_{\alpha i}$ .
4. Intrinsic alignments are embodied through the  $b^\kappa$ ,  $r^\kappa$ ,  $r^{g\kappa}$ , and  $r^{\kappa\kappa}$  coefficients.
5. Redshift-distribution errors are manifested through the uncertainties in the  $p_{\alpha i}$  probabilities.

The cost of this great generality is that there are a huge number of nuisance parameters, enough to make us doubt whether the maximum-likelihood analysis—or even the Fisher-matrix analysis!—is feasible.

## 2.7. Parameter Inventory

The WL survey covariance matrix has a horrendously large number of parameters. The cosmological treasure lies in these:

- The 2 global cosmological parameters  $\omega_m$  and  $\omega_k$ .
- The distances  $D_i$ , which encode the expansion history of the Universe in  $N_z$  steps. The  $\Delta\chi_i$  and the Hubble parameters  $h(z_i)$  can be expressed in terms of these and  $\omega_k$ .
- The metric-potential power spectra  $P_i^\phi$ , which describe the growth of dark-matter structure. For  $N_\ell$  bins in  $\ell$ , there will be  $N_\ell N_z$  distinct matter-power parameters in the model. A prediction for the growth of potential fluctuations will typically be an important element of any cosmological scenario under test, so the  $P_i^\phi$  can be replaced as parameters by a much smaller number of cosmological parameters.

There are then a large number of nuisance parameters. If there are  $N_{ss}$  non-empty source subsets, the nuisance parameters are

- The redshift-distribution parameters  $p_{\alpha i}$ , with  $N_{ss} - N_s$  degrees of freedom.
- The shear-calibration errors  $f_{\alpha i}$ , another  $N_{ss}$  degrees of freedom.
- The magnification-bias coefficients  $q_{\alpha i}$ , another  $N_{ss}$  degrees of freedom.
- The source-density biases  $b_{\alpha i}^g$  and correlation coefficients  $r_{\alpha i}^g$  with respect to  $\phi$ , which may be scale-dependent, yielding  $2N_\ell N_{ss}$  degrees of freedom.
- The intrinsic-alignment power and correlations with the mass,  $b_{\alpha i}^\kappa$  and  $r_{\alpha i}^\kappa$ , another  $2N_\ell N_{ss}$  parameters.
- The correlation coefficients  $r_{\alpha\beta i}^{gg}$ ,  $r_{\alpha\beta i}^{\kappa g}$ , and  $r_{\alpha\beta i}^{\kappa\kappa}$ , which also may be scale-dependent. The number of such parameters is  $\approx 3N_\ell N_{ss}^2/2N_z$ .

The number of nuisance parameters for a non-parametric analysis is enormous. If we are analyzing a photo-z survey with typical errors  $\Delta z \approx 0.05(1+z)$ , then we would typically want to space the redshift shells logarithmically in  $1+z$ , with  $\Delta \ln a \approx 0.02$  so that we resolve the redshift distribution of each photo-z bin. In this case,  $N_z \approx 100$  bins span  $0 < z < 5$ , and we will require  $N_{ss} \gtrsim 1000$  if we track all subsets out to  $\pm 3\sigma$  of the photo-z distribution.

To reduce the dimensionality of the likelihood function, we can replace many of the discrete nuisance parameters by the values of parameterized functions for the nuisance variables. Table 1 lists the variables in the WL likelihood function that can be replaced by parametric functions. The nuisance variables are functions of: wavevector  $k$ ; redshift  $z$ ; and redshift difference  $\Delta z = z_\alpha - z_i$  between the nominal and true redshifts of a source subset. In later sections we will describe the parametric functions that we have implemented to reduce the number of degrees of freedom in the model. Each time we introduce a parametric function, we need to choose a fiducial parameter set and a prior distribution for the parameters.

### 3. Spectroscopic Redshift Likelihood

If we draw a single member from source set  $\alpha$  and measure its spectroscopic redshift in an unbiased fashion, then by definition the likelihood of the spectroscopic redshift being on shell  $i$  is  $p_{\alpha i}$ . If we measure  $N_\alpha^{\text{spec}}$  redshifts, and find that  $N_{\alpha i}^{\text{spec}}$  are on shell  $i$ , then the likelihood is

$$\ln L = \sum_i N_{\alpha i}^{\text{spec}} \ln p_{\alpha i}. \quad (23)$$

This is true if the redshifts are statistically independent, which requires that they be dispersed across the sky to eliminate source correlations. We assume this limit.

Following Ma & Bernstein (2008), the Fisher matrix for the parameters  $\{p_{\alpha i}\}$  resulting from the unbiased spectroscopic observations is

$$F_{\alpha i \beta j} = \left\langle \frac{\partial^2 (-\ln L)}{\partial p_{\alpha i} \partial p_{\beta j}} \right\rangle = N_\alpha^{\text{spec}} \frac{\delta_{ij}}{p_{\alpha i}}. \quad (24)$$

We add this Fisher information to the density-lensing Fisher matrix (22) when considering the constraints offered by a WL survey that is combined with an *unbiased* spectroscopic redshift survey drawn from one or more of the source population sets.

We do not in general presume any functional form for the  $p_{\alpha i}$  redshift distributions when the sets are assigned from photo-z's. We adopt fiducial values either from an analytic form or from a simulation of photo-z performance. Then we leave all the  $p_{\alpha i}$  as free parameters in the Fisher matrix, adding the spectroscopic-survey Fisher matrix (24) if appropriate to the planned experiment. Note that the cross-correlations in the WL survey data offer constraints on the redshift distribution even if there is no unbiased spectroscopic survey ( $N_\alpha^{\text{spec}} = 0$ ).

## 4. An Implementation

A package of C++ classes implements the Fisher matrix calculation for Gaussian lensing+density observations, the spectroscopic-survey Fisher matrix, plus the models for lensing-potential power and nuisance functions described below. From these classes we can construct numerous applications, the most obvious being a Fisher-matrix forecast of cosmological constraints from the combination of a photometric galaxy lensing/density survey, plus a redshift survey to constrain the photo-z distribution. We list in Table 2 input fields for this forecasting implementation. Further program inputs are listed in later sections which detail the models for the lensing power spectrum and nuisance parameters that we describe below and adopt for this implementation.

In the current implementation we assume the source galaxies to be binned solely by photo-z, but generalizations are possible, *e.g.* including a second population of source galaxies sets that are observed spectroscopically. Note that when additional galaxy populations are introduced, we need a new set of nuisance functions to describe them. Furthermore, we need to model the cross-correlations between all galaxy populations.

The calculation of the Fisher matrix takes  $< 1$  minute per multipole bin using a single core of a typical current-epoch desktop CPU. Total execution time for a forecast is 10–20 minutes with the default parameters, with the most time-consuming operation being the marginalization over bias model parameters. The execution time is very sensitive to the redshift-shell width  $\Delta \ln a$  and to the width of the photo-z error distribution, as these control the number of subsets and the parameter count.

## 5. Power Spectrum Models

In most cosmological models, theory will offer strong guidance to the form of the lensing-potential power spectrum  $P^\phi(k, z)$ . In most forecasting or data-reduction codes this is a fully deterministic function of a small number of cosmological parameters. In our analysis, however, the theoretical prediction is taken as the mean  $P^\phi$  value of a prior distribution of finite uncertainty.

### 5.1. Central Model

The WL likelihood given above can be calculated for any model that predicts  $P^\phi$ . We have chosen to implement a model that allows for failure of General Relativity in describing growth of structure; but other models are possible if one wishes to test the Poisson equation or other tenets of General Relativity. Under the conditions

1. The potential and the mass-energy density are related by the Poisson equation of General Relativity, and

Table 1. Nuisance variables that can be replaced by functions

Description	Discrete variables	Parametric function
Lensing potential power spectrum	$P_i^\phi$	$P^\phi(k, z)$
Shear calibration error	$f_{\alpha i}$	$f(z, \Delta z)$
Magnification bias	$q_{\alpha i}$	$q(z, \Delta z)$
Redshift distribution	$p_{\alpha i}$	$p(z, \Delta z)$
Source density bias	$b_{\alpha i}^g$	$b^g(k, z, \Delta z)$
Density-mass correlation	$r_{\alpha i}^g$	$r^g(k, z, \Delta z)$
Intrinsic alignment bias	$b_{\alpha i}^\kappa$	$b^\kappa(k, z, \Delta z)$
IA-density correlation	$r_{\alpha i}^\kappa$	$r^\kappa(k, z, \Delta z)$
Density-density x-correlation	$r_{\alpha\beta i}^{gg}$	$r^{gg}(k, z, \Delta z_\alpha, \Delta z_\beta)$
Density-IA x-correlation	$r_{\alpha\beta i}^{g\kappa}$	$r^{g\kappa}(k, z, \Delta z_\alpha, \Delta z_\beta)$
IA-IA x-correlation	$r_{\alpha\beta i}^{\kappa\kappa}$	$r^{\kappa\kappa}(k, z, \Delta z_\alpha, \Delta z_\beta)$

Table 2. Controlling inputs to Fisher forecast

Parameter name	Description	Default
<code>fsky</code>	$f_{\text{sky}}$ , imaging sky coverage	0.5
<code>minLogL</code>	$\log_{10} \ell_{\text{min}}$ , minimum multipole	1.0
<code>maxLogL</code>	$\log_{10} \ell_{\text{max}}$ , maximum multipole	3.5
<code>logLStep</code>	$\Delta \log_{10} \ell$ , multipole bin width in dex	0.3
<code>zmax</code>	$z_{\text{max}}$ , redshift of most distant shell	3.5
<code>dlna</code>	$\Delta \ln a$ , width of distance shells	0.03
<code>coreDLna</code>	Maximum $ \ln(1 + z_i)/(1 + z_\alpha) $ of subsets	0.15
<code>sigGamma</code>	$\sigma_\gamma$ , shape noise per source galaxy	0.24
<code>zdist</code>	String specifying fiducial source $n_\alpha$ and $p_{\alpha i}$	...
<code>logNSpec</code>	$\log_{10} N_{\text{spec}}$	5.
<code>outfile</code>	Root name for output files	...

2. Non-relativistic matter is the only significant inhomogeneous component of the Universe, *i.e.* there is no dark-energy clustering, and
3. Matter is conserved,  $\bar{\rho}_m \propto a^{-3}$ , and
4.  $\Phi = -\Psi$ , as in the absence of anisotropic stress for General Relativity

then the potential power spectrum is related to the matter-density fluctuation spectrum  $P^m$  via

$$k^4 P^\phi(k, a) = \left( \frac{3\omega_m}{2a} \right)^2 P^m(k, a). \quad (25)$$

Under these conditions, the linearized perturbations to the metric grow in a scale-free manner so we can write

$$P_{\text{lin}}^\phi(k, a) = g_\phi^2(a) P_{\text{prim}}^\phi(k) T^2(k). \quad (26)$$

In our current code, the primordial power spectrum is a power law

$$\Delta_{\text{prim}}^2(k) \equiv \frac{k^3}{2\pi^2} P_{\text{prim}}^\phi(k) = \left( \frac{3\Delta_\zeta}{5} \right)^2 (k/k_0)^{n_s-1}. \quad (27)$$

The curvature variation  $\Delta_\zeta$  and spectral index  $n_s$  are free parameters. A running of the slope could easily be added. The normalization wavenumber  $k_0$  must be set by some convention. We typically adopt the 5-year WMAP parameters as fiducial values Komatsu et al. (2008).

The transfer function  $T(k)$  is taken from Eisenstein & Hu (1999). It is a function of the matter and baryon densities  $\omega_m$  and  $\omega_b$ . The impact of massive neutrinos could be added to the transfer function if desired. We ignore the baryon acoustic oscillations; experiments that try to exploit them will generate a distinct Fisher matrix for them.

The map from  $P_{\text{lin}}^\phi$  to the nonlinear  $P_{\text{nl}}^\phi$  is derived using the prescription of Smith *et al.* (2002) for nonlinear  $P^m$ , combined with the Poisson equation (25). The Smith *et al.* formula also requires knowledge of  $\Omega_m$  at the desired epoch, but it can be expressed in terms of other quantities that are already in our model:  $\Omega_m(z_i) = \omega_m a_i^{-3} h^{-2}(z_i)$ . We do not expect the Smith *et al.* (2002) formula to describe non-linear growth to high accuracy for all (or any) cosmologies. It does however capture the dependence of non-linear power on cosmological parameters to a level that suffices for forecasting purposes.

In General Relativity, the growth function  $g_\phi(a)$  is determined by the expansion history  $H(z)$ . Defining  $F = \ln(ag_\phi)$ , the growth equation is

$$F'' + (F')^2 + F' \left( 2 + \frac{d \ln h}{d \ln a} \right) = \frac{3\omega_m}{2h^2 a^3}, \quad (28)$$

where a prime denotes differentiation with respect to  $\ln a$ . Note that  $F'$  is the quantity  $d \ln g_m / d \ln a$  that appears in the peculiar-velocity power spectrum for a tracer of mass.

If GR holds, then the above relations fully specify the model for  $P^\phi$  given  $\{\omega_m, \omega_b, n_s, \ln \Delta_\zeta\}$  plus the expansion history, which in turn is given by  $\{D_i, \omega_k\}$ . As a test of GR, we allow the growth function arbitrary deviations from the  $F_{\text{fid}}$  that solves the GR growth equation for the fiducial expansion history:

$$\ln ag_\phi(a_i) = F_{\text{fid}}(a_i) + \delta F_i. \quad (29)$$

The  $\delta F_i$  become parameters of the likelihood function.

## 5.2. Model Errors

An important WL systematic is the expected finite accuracy in theoretical modeling of the power spectrum. We hence introduce an error function to describe the (logarithmic) difference between the power  $P^\phi$  and the value predicted by the parametric model described in the previous paragraphs:

$$\ln P^\phi(k, a) = \ln P_{\text{nl}}^\phi(k, a) + \delta \ln P(k, a). \quad (30)$$

The nuisance function  $\delta \ln P$  will be described with the “ $kz$ ” parametric form described in Appendix A. We parameterize the  $\delta \ln P$  function by its values  $\delta P_{ij}$  at a grid of points  $(k_i, a_j)$  regularly spaced in  $\ln k$  and  $\ln a$ . The  $\delta \ln P$  is linearly interpolated between grid points. The  $\delta P_{ij}$  become free parameters of the model and hence parameters in the likelihood function. We then place an independent Gaussian prior on each  $\delta P_{ij}$  which has mean of zero and a standard deviation of

$$\sqrt{\text{Var}(\delta P_{ij})} = 0.012 f_{\text{Zhan}} \begin{cases} 1 + 5 \log_{10}(k_i/k_1) & k_i > k_1 \\ (k_i/k_1)^{1+a_j} & k_i < k_1 \end{cases} \quad (31)$$

$$k_1 \equiv a^{-2.6} \text{Mpc}^{-1}. \quad (32)$$

This function is a fit to an estimate, supplied by Hu Zhan, of the impact of baryonic physics on the mass power spectrum Zhan & Knox (2004); Jing *et al.* (2006). We scale the overall size of the theory-error systematic with the control scalar  $f_{\text{Zhan}}$ . We can also adjust the density  $\Delta \ln k$  and  $\Delta \ln a$  at which the  $\delta P_{ij}$  grid points are spaced. This corresponds to setting some coherence length for theory errors in this space. In §7 we will investigate the choice of these grid spacings.

The procedure above means that we replace the  $P_i^\phi$  as parameters in our likelihood with a new (and hopefully smaller) set:

- The small set  $\{\omega_m, \omega_b, \Delta_\zeta^2, n_s\}$  that control the linear power spectrum.
- The  $\{\delta F_i\}$  which define the growth function vs redshift.
- A grid of theory error values  $\delta P$ , which are nuisance parameters to marginalize after construction of a Fisher matrix or likelihood. We have physically-based priors to apply to these before marginalization.

Table 3 lists the input fields for the part of our forecasting code which constructs the power-spectrum model. The WMAP5  $\Lambda$ CDM cosmology provides the fiducial values of all lensing power values; the program inputs define the behavior of the deviations from the theoretical model and the prior expectations on the size of such deviations.

## 6. Non-parametric nuisance modeling

### 6.1. General comments on nuisance functions

The WL likelihood contains many nuisance parameters that are discretized representations of nuisance *functions*. It is common in the literature to assign some parametric form to a nuisance function, then marginalize over the parameters of the nuisance function to recover a purely cosmological likelihood. This can be a very dangerous approach: if the nuisance function does *not* in actuality follow the assumed form, then the process is invalid and we may have greatly overestimated the power of the experiment to remove the systematic error from the signal. When marginalizing over a systematic, we must be sure that the assumed parametric form is sufficiently flexible to include any expected manifestation of the systematic. For example we should not assume that systematics scale linearly with redshift unless there is a physical reason to expect this.

It is unfortunately not possible to model a completely free function with a finite number of free parameters. This becomes possible, however, if we limit the bandwidth of variation in the function. As an example consider our power-spectrum theory error function  $\delta \ln P(k, z)$ . We could decompose  $\delta \ln P$  into Fourier modes or polynomial terms over its finite  $(k, z)$  domain. Retaining a finite number of modes or terms leads to a tractable parameterization, albeit with a maximum frequency or polynomial order that defines a coherence length for the reconstructed function. For  $\delta \ln P$  we choose to limit the bandwidth using linear interpolation between a 2d grid of specified values. In Appendix A we describe the family of functions that we use to model the nuisance functions of  $(k, z, \Delta z)$  that are common in the WL likelihood analysis (*cf.* Table 1).<sup>1</sup> The Appendix

---

<sup>1</sup> In practice we use  $\ln a$  and  $\Delta \ln a$  to specify each subset’s nominal redshift and redshift error, but in the text we will stick with  $(z, \Delta z)$  to reduce the clutter.

Table 3. Power spectrum inputs to Fisher forecast

Parameter name	Description	Default
<code>zhan</code>	$f_{\text{Zhan}}$ , power-spectrum theory uncertainty relative to baryonic effects	0.5
<code>psDlnk</code>	$\Delta \ln k$ , node spacing of power-spectrum theory errors in $k$	1.0
<code>psDlna</code>	$\Delta \ln a$ , node spacing of power-spectrum theory errors in $a$	0.5

describes both the functional form, and the prior likelihoods on the parameters that are used to give the nuisance function the desired *RMS* uncertainty.

These models of nuisance functions are non-parametric in the sense of being able to reproduce very general types of behavior once the bandwidth is specified. The question remains: what is the proper choice of bandwidth to allow the nuisance function? Our approach is to find the bandwidth which *causes the most damage to cosmological constraints* under a prior that specifies the expected RMS fluctuations in the nuisance function. This is the most conservative approach. Typically one finds the following: if the nuisance function is given a highly coherent, low-order functional form, then it is easily distinguished from cosmological signals and can be marginalized away with little damage to cosmological constraints. On the other hand if the nuisance-function bandwidth is very high, then the broad WL kernel tends to average away the nuisance signal, leaving little trace in the cosmology. There is an intermediate point where the systematic error is most easily confused with cosmology. The conservative approach is to find this regime and use it for modeling the systematic error. In §7 we will find coherence lengths in  $z$  and  $k$  at which our systematics are most damaging.

## 6.2. Redshift Distributions

We specify the fiducial values of the photo- $z$  distribution  $n_\alpha$  and error probabilities  $p_{\alpha i}$  either with analytic formulae (*e.g.* photo- $z$  errors Gaussian in  $\ln a$ ), or by taking the output of a simulation of galaxy detection and photo- $z$  assignment for the chosen survey. For spectroscopic samples or the CMB source plane there are no photo- $z$  errors at all.

We do not place any parametric form or prior assumption on the  $p_{\alpha i}$ . All redshift constraints arise either from the lensing survey data itself or from additional spectroscopic data. The likelihood arising from spectroscopic redshift samples is described in §3.

## 6.3. Shear calibration and magnification bias

The shear calibration factors  $f_{\alpha i}$  and magnification bias coefficients  $q_{\alpha i}$  are, most generally, distinct in every subset. We use the “ $z\Delta z$ ” functional form described in Appendix A to generate the  $f_{\alpha i}$  and  $q_{\alpha i}$  from a smaller set of function parameters. Each function is specified by a polynomial function of  $\Delta z$ ; polynomial coefficients are interpolated between grid points equally spaced in  $\ln a$  at intervals  $\Delta \ln a$ .

We set the fiducial functions to be  $f_{\alpha i} = 0$ , and  $q_{\alpha i} = q_{\text{fid}}$  independent of  $(k, z)$ . The priors on the polynomial coefficients are chosen to yield a chosen RMS variation of  $f$  or of  $q$ . As detailed in Appendix A, we also specify whether the nuisance function varies mostly along the  $z$  direction or along the  $\Delta z$  direction of its domain.

Table 4 lists the program inputs necessary to specify the model for  $f$  or  $q$ : their functional

form, fiducial values, and priors on deviations from the fiducial.

#### 6.4. Galaxy correlation coefficients

The correlation coefficient  $r_{\alpha i}^g$  is, most generally, different at each subset and at each multipole  $\ell$ . We model  $r^g$  using the “ $kz\Delta z$ ” function form described in Appendix A. These functions are polynomial in  $\Delta z$ , with the polynomial coefficients linearly interpolated from a grid in  $(\ln k, \ln a)$  space. This grid of polynomial coefficients replaces the  $r_{\alpha i}^g$  as parameters in the likelihood.

For the fiducial correlation coefficient, we interpolate smoothly between a linear and non-linear limit according to the value of  $\Delta_{\text{lin}}^2(k, z) = k^3 P_{\text{lin}}^m(k, z)/2\pi^2$ :

$$r_{\text{fid}}^g(k, z) = \frac{r_{\text{NL}}^g + r_{\text{L}}^g}{2} + \frac{(r_{\text{NL}}^g - r_{\text{L}}^g)}{\pi} \tan^{-1} \left[ \frac{\ln \Delta_{\text{lin}}(k, z)}{W} \right]. \quad (33)$$

The constant  $W$  sets the width of the transition from the linear to nonlinear regime. We set  $W = 1$  unless otherwise noted.

Each polynomial coefficient at each grid point is assigned an independent Gaussian prior. These are selected to yield a preselected RMS variation  $r_{\text{RMS}}^g$ . The RMS prior uncertainties are interpolated in  $(k, z)$  space between linear and non-linear limiting values  $r_{\text{RMS,L}}^g$  and  $r_{\text{RMS,NL}}^g$  using the same functional form (33).

Table 5 lists the program inputs needed to specify the galaxy bias and correlation models.

#### 6.5. Galaxy bias

We expect  $b^g$  to vary quite strongly with  $z$ , as the more distant source galaxies are likely intrinsically very bright and highly biased. There may also be a strong dependence of  $b^g$  on  $\Delta z$

Table 4. Shear calibration and magnification bias inputs to Fisher forecast

Parameter name	Description	Default
fRMS	$f_{\text{RMS}}$ , RMS variation of $f$ allowed under prior	0.01
qFid	$q_{\text{fid}}$ , fiducial value for all $q_{\alpha i}$	1.0
qRMS	$q_{\text{RMS}}$ , RMS variation of $q$ allowed under prior	0.1
fqDlna	$\Delta \ln a$ , node spacing for $f$ & $q$ models	0.5
fqDzOrder	Order of polynomial used to model $\Delta z$ dependence of $f, q$	2
fqVarFracDZ	Fraction of $f, q$ variance that due to $\Delta z$ dependence	0.5

because both  $\Delta z$  and the bias may couple strongly to galaxy spectral type. Variation with  $k$  should be weaker. We hence define  $b^g$  to be the sum of two functions,

$$b^g = b_{\text{coarse}}^g(z, \Delta z) + b_{\text{fine}}^g(k, z, \Delta z). \quad (34)$$

The fiducial values are  $b_{\text{coarse}}^g = b_{\text{fid}}^g, b_{\text{fine}}^g = 0$ .

The coarse contribution is given a very weak prior, but can only vary slowly with  $z$ :  $\Delta \ln a = 0.5$  by default for the  $b_{\text{coarse}}^g$  grid nodes.

The  $b_{\text{fine}}^g$  function is interpolated between the same  $(\ln k, \ln a)$  grid points as the correlation coefficient  $r^g$ . The prior on each  $b_{\text{fine}}^g$  node is arranged to give RMS uncertainty that is interpolated between linear and nonlinear limits  $b_{\text{RMS,L}}^g$  and  $b_{\text{RMS,NL}}^g$  just as for  $r^g$ .

## 6.6. Intrinsic Alignments

The strength of intrinsic alignments are specified by the  $b_{\alpha i}^\kappa$  and  $r_{\alpha i}^\kappa$  values at each multipole  $\ell$ . As for the galaxy density, the free-parameter count can be reduced by specifying parametric functions  $b^\kappa, r^\kappa$  of  $(k, z, \Delta z)$  instead. Each of these two functions modeled using the “ $kz\Delta z$ ” form described in Appendix A, just as for  $r^g$ . The fiducial  $b_{\text{fid}}^\kappa$  and  $r_{\text{fid}}^\kappa$  are taken as constant over the entire domain. The RMS variation  $b_{\text{RMS}}^\kappa$  and  $r_{\text{RMS}}^\kappa$  in the priors of these functions are also taken to be constant over the domain. We take  $b_{\text{RMS}}^\kappa = |b_{\text{fid}}^\kappa|$ , because we expect that the best constraints on IA to always arise from self-calibration of WL surveys rather than through any external modeling or prior. Roughly speaking, the IA measured by Mandelbaum et al. (2006) for the SDSS population corresponds to  $b^\kappa \approx -0.003$  (Bridle & King 2007), which we will normally take as our fiducial model for IA. Setting  $b_{\text{fid}}^\kappa = 0$  turns off the IA systematic entirely.

Table 6 lists the program inputs needed to specify the functional form for intrinsic alignments, the fiducial values, and the prior constraints. Note that we assume the intrinsic-alignment functions to be defined on the same  $(\ln k, \ln a)$  grid as the galaxy bias and covariance functions.

## 6.7. Cross-correlation coefficients

The cross-correlation coefficients  $r_{\alpha\beta i}^{gg}, r_{\alpha\beta i}^{g\kappa}$ , and  $r_{\alpha\beta i}^{\kappa\kappa}$  are even more complex because each depends on  $k, z$ , plus two subsets’  $\Delta z_{\alpha i}$  and  $\Delta z_{\beta i}$ . We find it infeasible to construct nuisance-function templates spanning 4 dimensions. We therefore simplify by first writing

$$r_{\alpha\beta i}^{g\kappa} = r_{\alpha i}^g r_{\beta i}^\kappa + s_{\alpha\beta i}^{g\kappa} \sqrt{[1 - (r_{\alpha i}^g)^2] [1 - (r_{\beta i}^\kappa)^2]}. \quad (35)$$

A value  $|s_{\alpha\beta i}^{g\kappa}| \leq 1$  is necessary (but not sufficient) to keep the mass-galaxy covariance matrix from acquiring non-physical negative eigenvalues. In principle the functional form of  $s^{g\kappa}$  must vary

Table 5. Galaxy bias inputs to Fisher forecast

Parameter name	Description	Default
bg	$b_{\text{fid}}^g$ , fiducial galaxy bias	1.5
rgL	$r_{\text{L}}^g$ , fiducial galaxy correlation coeff at linear limit	0.9
rgNL	$r_{\text{NL}}^g$ , fiducial galaxy correlation coeff at non-linear limit	0.6
biasDlnk	$\Delta \ln k$ interpolation grid step for bias models	1.0
biasDlna	$\Delta \ln a$ interpolation grid step for bias models	0.1
brgRMSL	$b_{\text{RMS,L}}^g$ and $r_{\text{RMS,L}}^g$ RMS prior variation for bias and correlation, linear limit	0.05
brgRMSNL	$b_{\text{RMS,NL}}^g$ and $r_{\text{RMS,NL}}^g$ RMS prior variation non-linear limit	0.10
brVarFracDZ	Fraction of $b^g, r^g$ variance due to $\Delta z$ dependence	0.2
bgCoarseDlna	$\Delta \ln a$ node grid spacing for $b_{\text{coarse}}^g$	0.5
bgCoarseZRMS	RMS prior variation of $b_{\text{coarse}}^g$ at $\Delta z = 0$	0.5
bgCoarseDZRMS	RMS prior variation of $b_{\text{coarse}}^g$ at fixed $z$	0.3
kgg	$K_{\text{fid}}^{gg}$ , fiducial value of $K^{gg}(k, z)$ cross-corr spec	2.
kggRMS	$K_{\text{RMS}}^{gg}$ , prior variation on $K^{gg}(k, z)$	1.

Table 6. Intrinsic-alignment (IA) inputs to Fisher forecast

Parameter name	Description	Default
bk	$b_{\text{fid}}^\kappa$ , fiducial intrinsic alignment	−0.003
rk	$r_{\text{fid}}^\kappa$ , fiducial correlation between mass and intrinsic alignment	0.7
rkRMS	$r_{\text{RMS}}^\kappa$ , RMS prior variation in $r^\kappa$	0.2
kkk	$K_{\text{fid}}^{\kappa\kappa}$ , fiducial value of $K^{\kappa\kappa}(k, z)$	1.
kkkRMS	$K_{\text{RMS}}^{\kappa\kappa}$ , RMS prior variance of $K^{\kappa\kappa}$	1.
skg	$s_{\text{fid}}^{g\kappa}$ , fiducial IA-bias cross-correlation	0.
skgRMS	$s_{\text{RMS}}^{g\kappa}$ , RMS prior on IA-bias cross-correlation	0.3

over four dimensions, but we make the gross simplification that it is constant for the survey, since we expect this type of cross-correlation to have minimal effect on cosmological constraints. The program thus requires simply a fiducial scalar  $s^{g\kappa}$  and an RMS for its Gaussian prior.

The density-density cross-correlation  $r^{gg}$  may have substantial impact on cosmological constraints, so we model it with more freedom, though not full 4-dimensional behavior. We set

$$s_{\alpha\beta i}^{gg} = \max \left[ 0, 1 - K^{gg}(k, z_i) \frac{|z_\alpha - z_\beta|}{2\Delta z_{\max}} \right]. \quad (36)$$

This functional form for  $s$  gives the most closely related subsets the highest covariance.  $\Delta z_{\max}$  is the width of the redshift distribution within a set. The function  $K^{gg}(k, z)$  adjusts how quickly the subsets decorrelate as their photo- $z$ 's diverge.  $K^{gg}(k, z)$  is implemented as the “ $kz$ ” functional form described in Appendix A, namely a linear interpolation between a grid of values in the  $(\ln k, \ln a)$  plane. We hence parameterize the 4-dimensional cross-correlation function by a 2d grid of  $K^{gg}$  nodal values. These points are all given the same fiducial value  $K_{\text{fid}}^{gg}$ . The  $K^{gg}$  nodal values are given Gaussian priors to select a range of uncertainty  $K_{\text{RMS}}^{gg}$ .

The cross-correlation parameters  $r_{\alpha\beta i}^{\kappa\kappa}$  are similarly reduced from 4-dimensional behavior by defining values  $s_{\alpha\beta i}^{\kappa\kappa}$  that are set by the nodal values of a 2-dimensional function  $K^{\kappa\kappa}(k, z)$  in complete analogy with Equation (36).

## 6.8. An apology

This section on nuisance functions is obscure and lengthy, especially regarding the cross-correlations of galaxies and intrinsic alignments. It is, unfortunately, impossible to fully describe the likelihood of lensing survey data without invoking some model for all of these functions.

Previous work has avoided these messy details and functions by making many simplifications. Most have implicitly assumed that all the correlation coefficients are unity. Most have ignored the intrinsic-alignment signal entirely, *i.e.* taking  $b^\kappa = 0$ . All previous analyses have considered the galaxy bias to be constant within a set, and if the multiplicative error has been considered, it has also been constant within a galaxy set. Only a few analyses have allowed galaxy bias to vary with redshift (Zhan 2006; Bernstein & Jain 2004). The most sophisticated treatment to date is that of Hu & Jain (2004), who take all bias and correlation coefficients to derive from a halo model of galaxies. The redshift-distribution parameters  $p_{\alpha i}$  have, in the most ambitious analyses to date, been reduced to two-parameter (Gaussian) functions. Ma & Bernstein (2008) consider sum-of-Gaussian models. These assumptions can all be implemented in the present formalism if desired, but can also be relaxed to assess their impact on the cosmological constraints.

## 7. Tuning the forecast parameters

In this section we determine the values of bin widths and nuisance-function bandwidths that are needed for reliable extraction of maximum information from lensing surveys. Unless otherwise noted, we will derive these parameters for a canonical survey with  $f_{\text{sky}} = 0.5$ ; an effective source density of 60 galaxies per arcmin<sup>2</sup> with median redshift of 1.2;  $\sigma_\gamma = 0.24$ ; and Gaussian-distributed fiducial photo-z errors of  $\sigma_z = 0.04(1+z)$ . Except as noted, we assume  $N_{\text{spec}} = 10^7$  so that photo-z calibration errors are negligible, and also reduce the shear calibration RMS uncertainty to  $10^{-4}$  to be negligible as well. Other inputs assume the default values given in Tables 2–6.

The information content of a survey will be gauged using the DETF figure of merit (Albrecht et al. 2006): the Fisher matrix will be marginalized over all nuisance parameters, then the  $D_i$  and  $\delta F_i$  variables projected onto a model obeying General Relativity with homogeneous dark energy of equation of state  $w = w_0 + w_a(1-a)$ . A prior representing expected Planck results is added (also from the DETF report), and we marginalize over  $\{\omega_m, \omega_b, \omega_k, \omega_{\text{DE}}, n_s, \Delta_\zeta\}$  to yield the Fisher matrix  $\mathbf{F}_w$  over  $\{w_o, w_a\}$ . The DETF FoM is defined as  $|\mathbf{F}_w|^{1/2}$ .

### 7.1. Multipole bin size

Since we have excluded baryon oscillations from our transfer function, we expect to find little information in the detailed shape of the lensing or density power spectra. The broad lensing kernel in redshift also smoothes away fine structure in the convergence. So we expect the information content in the Fisher matrix to be independent of the multipole bin width  $\Delta \log_{10} \ell$  below some modest value. Larger values of  $\Delta \log_{10} \ell$  reduce the complexity and execution time of the calculations, so we seek the maximum  $\Delta \log_{10} \ell$  at which nearly all the lensing information is present.

Figure 1 plots the DETF FoM of the lensing+density survey (plus spectroscopic redshift survey and Planck prior) vs  $\Delta \log_{10} \ell$  for several candidate surveys. The top line is for a very optimistic survey:  $n_{\text{eff}} = 100 \text{ arcmin}^{-2}$ ,  $N_{\text{spec}} = 10^7$ ,  $q_{\text{RMS}} = 10^{-3}$ ,  $f_{\text{RMS}} = 10^{-4}$ ,  $b_{\text{RMS}}^g = r_{\text{RMS}}^g = 0.01$ , and  $b_{\text{fid}}^\kappa = 10^{-3}$ . By reducing the systematics and the shot noise to (unrealistically) low levels, we give the lensing survey the chance to extract maximal information. We find that the FoM gains only 2% for  $\Delta \log_{10} \ell < 0.3$ .

Other lines in the plot are FoM vs  $\Delta \log_{10} \ell$  for weaker surveys, with  $N_{\text{spec}} = 10^{4.5}$  and/or  $n_{\text{eff}} = 60 \text{ arcmin}^{-2}$ ,  $q_{\text{RMS}} = 0.1$ ,  $b_{\text{RMS}}^g = r_{\text{RMS}}^g = 0.1$ ,  $b_{\text{fid}}^\kappa = -0.003$ . In these cases we also find that the DETF FoM increases by  $< 2\text{--}3\%$  for  $\Delta \log_{10} \ell < 0.3$ .

We adopt  $\Delta \log_{10} \ell = 0.3$  for all future use.

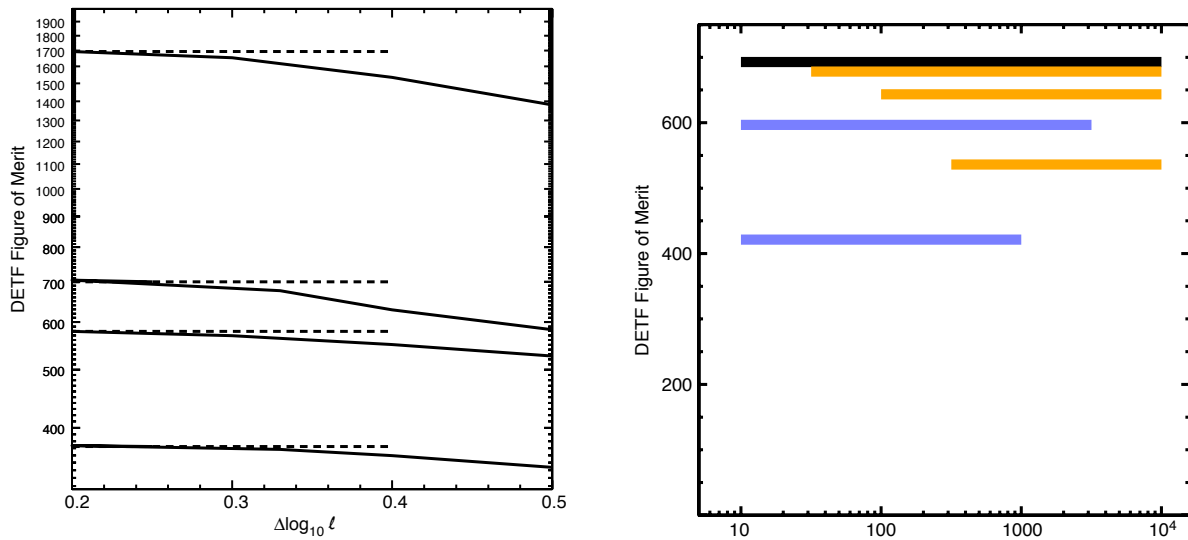


Fig. 1.— *Left*: DETF Figure of Merit resulting from Fisher analyses of several weak lensing surveys, plotted against multipole bin width  $\Delta \log_{10} \ell$  of the analysis. Each solid line plots a particular survey scenario (see text for details). The dashed lines are horizontal, to help the eye judge the information degradation as we increase  $\Delta \log_{10} \ell$ . We conclude that  $\Delta \log_{10} \ell \leq 0.3$  retains  $> 97\%$  of the information for surveys of any quality level. *Right*: Value of DETF FoM for the default survey vs range of multipole used. Choice of upper bound is more critical than choice of lower bound on  $\ell$ .

## 7.2. Multipole range

On the right-hand side of Figure 1 we plot the DETF FoM for various ranges of  $\ell$ . In this study we assume a space based survey obtaining  $n_{\text{eff}} = 60 \text{ arcmin}^{-2}$  over  $f_{\text{sky}} = 0.5$ . The photo- $z$  and shear calibration systematics are held negligible with priors but other systematics (intrinsic alignment, etc.) have default priors.

We see that the choice of  $\ell_{\text{max}}$  has a strong influence, as moving from  $10^3$  to  $10^4$  changes the FoM by  $1.7\times$ . We note this is true even though we have included uncertainty in the theoretical power spectrum at high  $k$  values, showing that there is still information to be gained when the theory is incomplete. We find, in fact, that our default power-spectrum theory uncertainty of  $f_{\text{Zhan}} = 0.5$  leads to only 6% degradation of the DETF FoM relative to an assumption of *zero* uncertainty in the theory, even when  $\ell_{\text{max}} = 10^4$ .

Unfortunately our assumption of Gaussian statistics will fail by  $\ell = 10^4$  Cooray & Hu (2001); Lee & Pen (2008), rendering the Fisher calculation less reliable. We will restrict our analysis to  $\ell < 10^{3.5}$ , but additional study of the effect of non-Gaussian statistics is clearly needed.

The flat-sky and Limber approximations will fail at low  $\ell$ , but the choice of  $\ell_{\text{min}}$  appears less critical to the  $w_0/w_a$  information content, so will retain the  $\ell > 10$  bound in our analyses.

## 7.3. Scale resolution for nuisance functions

We require choice of node spacing  $\Delta \ln k$  in the nuisance functions for the power-spectrum theory errors, the calibration errors  $f$  and  $q$ , and the bias/correlation parameters  $b_{\text{fine}}^g, r^g, b^\kappa, r^\kappa, K^{gg}$ , and  $K^{\kappa\kappa}$ . We set  $\Delta \ln k$  to be equal for all nuisance functions, and find the value which minimizes the DETF FoM as the “most damaging” scale of variation. We examine the default case described above, for several values of the shear calibration prior  $f_{\text{RMS}}$  and photo- $z$  calibration size  $N_{\text{spec}}$ .

Figure 2 shows  $\Delta \ln k \approx 0.7\text{--}1$  yields minimum information for fixed RMS priors, but the dependence is very weak. The FoM varies by only 7% over the range  $0.5 < \Delta \ln k < 1.5$ . We henceforth adopt  $\Delta \ln k = 1$ . Perhaps not surprisingly, this makes the nuisance functions have  $\approx 1$  independent node in each multipole bin of  $\Delta \log_{10} \ell = 0.3$ .

## 7.4. Redshift resolution for nuisance functions

All of the nuisance functions are dependent on  $z$ . We next investigate the redshift node spacing  $\Delta \ln a$  at which the nuisance functions are most damaging to the DETF FoM. We find that the FoM is insensitive to the  $\Delta \ln a$  of the power-spectrum theory errors. The value of  $\Delta \ln a$  for the calibration functions  $f$  and  $q$  that minimizes the FoM depends upon the strength of the prior. The choice  $\Delta \ln a = 0.5$  produces a FoM that is within 2% of the minimum, however, so we fix this value

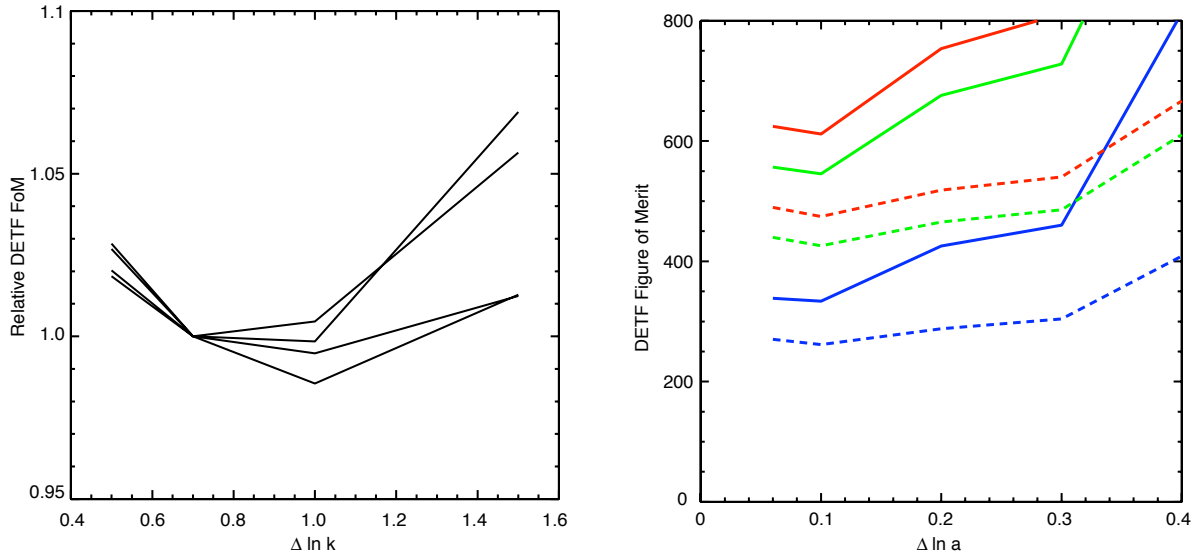


Fig. 2.— *Left:* DETF FoM vs  $\Delta \ln k$ , the spacing of nuisance-function nodes in the length-scale axis. We examine surveys with varying strengths of priors on shear calibration and photo- $z$  calibration. For this plot, each is normalized to the value at  $\Delta \ln k = 0.7$  in order to show the (weak) dependence of FoM on  $\Delta \ln k$  when the prior on RMS nuisance-function fluctuations are held fixed. We adopt  $\Delta \ln k = 1$  as the most conservative bandwidth for nuisance-function variation with scale. *Right:* DETF FoM vs  $\Delta \ln a$ , the spacing of nodes in redshift for the bias, correlation, and intrinsic-alignment nuisance functions. The FoM is quite sensitive to this choice, and allowing the bias/IA to vary on  $\Delta \ln a = 0.1$  scales is most damaging to cosmological inference.

for the theory-error and calibration nuisance functions.

The redshift freedom given to the bias and intrinsic-alignment nuisance functions has a strong impact on the DETF information content. Figure 2 illustrates that, at fixed RMS prior variation, models with freedom to vary on rather fine scales,  $\Delta \ln a = 0.1$  are most damaging to cosmological information.

## 8. Conclusion

The core of this paper are the expressions (18)–(20) for the two-point correlation matrix of the lensing and density observable multipoles produced by a typical lensing survey. This was derived under a very limited set of assumptions: a homogeneous and isotropic 4-dimensional metric Universe with scalar perturbations; plus the weak-lensing limit, the Limber and Born approximations, and an approximation that lensing magnification bias and intrinsic density fluctuations are additive. The last four assumptions could be relaxed at the expense of computational complexity. We thus hope that data analyses based on this framework could be used to constrain a wide variety of potential explanations for the acceleration phenomenon, including gravity modifications as well as new fields in the Universe. In the limit of Gaussian fluctuation fields, the two-point information is a complete description of the likelihood and hence can be used to construct Fisher matrices or analyze data. As currently configured, the analysis yields the survey’s ability to constrain the distance function  $D(z)$  and linear growth function  $g_\phi(z)$ , without reference to particular dark-energy models. It would be straightforward to implement scale-dependent linear-growth functions.

This framework subsumes all of the information (up to 2-point level) that is likely to be obtained from lensing observations: density-density, lensing-density, and lensing-lensing correlations, plus redshift distributions from unbiased spectroscopic surveys (§3). Furthermore it allows for the most important expected forms of systematic error: photo- $z$  calibration errors, shear and magnification-bias calibration errors, intrinsic alignments, and inaccuracies in power-spectrum theory. Systematics that are additive to shear (*e.g.* uncorrected PSF ellipticity) or to density (*e.g.* uncorrected foreground extinction) have not been included. We have not done so since the additive errors could, in principle, exhibit almost any arbitrary signature in the covariance matrix of the observables. Hence a completely general model for additive errors would be degenerate with almost all other signals. For the additive systematics, it is better to determine the level at which they would bias the cosmological results than to attempt to fit a model. Amara & Refregier (2007) is a good example of this approach.

Since the analysis framework is independent of models for dark energy, gravity, power-spectrum evolution, or galaxy bias, we get a stripped-down look at what parameters are truly constrained by the data, and what nuisance functions must be modeled in order to extract the cosmological information. There is a substantial suite of biases and correlation functions involved in understanding the full survey data. In other work these have been ignored, or have been quantified by

reference to halo occupation models (Hu & Jain 2004; Cacciato *et al.* 2008). Here we introduce generic functions for bias and calibration nuisance functions that are not based on any particular physical model.

We implement one possible model for the evolution of the lensing-potential power spectrum, based on General Relativity but allowing for failure of the growth equation. It is straightforward to implement other potential deviations from General Relativity. In the current implementation, the end result of the Fisher analysis is a forecast of the ability to constrain the functions  $D_A(z)$  and  $g_\phi(z)$ .

Since the analysis must be discretized in redshift and angular scale in order to be feasible, we investigated the bin sizes or bandwidths of nuisance functions that should be chosen. We find that  $\approx 3$  bins per decade of angular scale suffice to extract all information (apart from baryon acoustic oscillations), and that nuisance functions should be specified no finer than this. Nuisance functions for power-spectrum theory errors and for shear and magnification-bias calibration errors can be specified coarsely in redshift space ( $\Delta \ln a \approx 1$ ), but the galaxy biases, correlations, and intrinsic-alignments must be modeled with potentially finer structure in redshift ( $\Delta \ln a \approx 0.1$ ) to immunize against potential astrophysical systematics.

In future papers we will use this framework and its implementation to investigate the requirements for spectroscopic calibration of photo- $z$ 's in large lensing surveys, and other practical issues. As a simple first application of our framework, we have shown here that power-spectrum theory uncertainty does not significantly degrade the cosmological power of a nominal lensing survey at  $10 < \ell < 10^4$ . Non-Gaussian statistics are a much more important factor to consider.

**C++** Code to implement Fisher forecasting using this framework has been written and runs quickly on desktop computers despite the large number of free parameters in these general models. Interested parties should contact the author for access to the code.

This work is supported in this work by grant AST-0607667 from the National Science Foundation, Department of Energy grant DOE-DE-FG02-95ER40893, and NASA grant BEFS-04-0014-0018. I thank Bhuvnesh Jain, Zhaoming Ma, Chris Hirata, Ravi Sheth, Hu Zhan, and the members of the Dark Energy Task Force for helpful conversations during the long gestation of this work.

## A. Parametric functional forms for nuisance variables

In modeling an experiment, we often encounter some systematic error associated with a nuisance variable  $f$  about which we have little *a priori* knowledge. We would like to fit some parametric form to this variable, but would like a form that is flexible enough to describe any “reasonable” behavior the function might exhibit. We also want to conveniently relate the number and prior probabilities for the parameters to the kind of variation that  $f$  might exhibit. A parametric de-

scription of some nuisance function  $f$  defined over a variable  $x \in [-1, 1]$  would ideally have the following properties:

1.  $f(x)$  has a variable number  $N$  of controlling parameters  $\{a_0, a_2, \dots, a_{N-1}\}$  such that any continuous differentiable function  $F(x)$  can be approximated to any desired accuracy with a sufficiently large choice of  $N$ .
2. We can draw  $\{a_j\}$  from independent Gaussian distributions of zero mean and widths  $\{\sigma_j\}$ , with the result that  $\text{Var}[f(x)]$  is independent of  $x$ . In other words, the nuisance value  $f$  has a uniform and well-determined variance when we apply a simple diagonal Gaussian prior to the parameter set  $\{a_j\}$ .

A Fourier decomposition,  $f = \sum(a_j \sin j\pi x + b_j \cos j\pi x)$ , exhibits these qualities, but converges poorly when  $f(-1) \neq f(+1)$ .

### A.1. Linearly interpolated functions

Another approach is linear interpolation: choosing a spacing  $\Delta x = 2/(N - 1)$ , we define  $a_i$  as the value of  $f$  at  $x_i = i\Delta x - 1$ . At some other  $x_i < x < x_{i+1}$ , we define

$$f(x) = wa_i + (1 - w)a_{i+1}, \quad w = \frac{x_{i+1} - x}{\Delta x}. \quad (\text{A1})$$

If we assign an independent Gaussian prior of width  $\sigma_a$  to each  $a_i$ , then by definition we have  $\text{Var}[f(x)] = \sigma_a^2$  if  $x$  coincides with a node. But the variance of  $f$  is not quite homogeneous: it drops to  $\text{Var}[f(x)] = \sigma_a^2/2$  when  $x$  is halfway between two nodes. If we want the *mean* variance of  $f(x)$  over the interval  $x \in [-1, 1]$  to equal  $\sigma_f^2$ , then the variance of the prior on each node needs to be  $\sigma_a^2 = 3\sigma_f^2/2$ .

### A.2. Legendre polynomials

Polynomial expansions are also commonly used to model nuisance functions. The simplistic form  $f(x) = \sum a_i x^i$  results in extremely non-uniform variance for  $f$  with diagonal prior on  $\{a_i\}$  and is hence inappropriate for our purpose. A better choice is to expand in Legendre polynomials  $P_n(x)$ , which are orthogonal over  $[-1, 1]$ . We define

$$f(x) = \sum_{i=0}^{N-1} a_i P_i(\nu x). \quad (\text{A2})$$

Recall that the Legendre polynomials satisfy  $P_0 = 1, P_1 = x, (n + 1)P_{n+1} = (2n + 1)xP_n - nP_{n-1}$ .

We wish to choose priors  $\{\sigma_i\}$  on  $\{a_i\}$  that cause the variance of  $f(x)$  be as uniform as possible for  $x \in [-1, 1]$ . We have not found a way to attain perfect uniformity in  $x$  with polynomial interpolation, however the following scheme gets usefully close. We discover numerically that

$$\lim_{N \rightarrow \infty} \frac{1}{N} \sum_{i=0}^{N-1} P_n^2(\nu x)(2i+1) = \frac{2}{\pi} (1 - \nu^2 x^2)^{-1/2}. \quad (\text{A3})$$

This implies that, if we set  $\sigma_i = \sqrt{(2i+1)\pi/2N}$ , then in the limit of large  $N$  we will obtain  $\text{Var}[f(x)] = (1 - \nu^2 x^2)^{-1/2}$ . For  $\nu = 1$  this would diverge at the ends of our nuisance function's interval. If, however, we choose  $\nu = 0.9$ , the RMS is only  $\approx 1.5\times$  larger at the endpoints than at  $x = 0$ . Over the  $[-1, 1]$  interval, the mean variance is  $(\sin^{-1} \nu)/\nu$ . Hence if we wish to have a function with  $\langle \text{Var} f(x) \rangle_x = \sigma_f^2$ , we set the priors on the Legendre coefficients to be

$$\sigma_i = \sigma_f \sqrt{\frac{(2i+1)\pi\nu}{2N \sin^{-1} \nu}}. \quad (\text{A4})$$

### A.3. Standard multidimensional functions

The Fourier, linear-interpolation, and Legendre-polynomial functional forms can each be extended to  $> 1$  dimensions in straightforward fashion. In the lens modeling, we need functions of these dimensions:

1. Comoving wavenumber or physical scale:  $x_1 = \ln k$ ;
2. Redshift  $z$ : more precisely we will use the variable  $x_2 = \ln(1+z)$ ;
3. Photometric redshift error  $\Delta z$ ; more precisely, our code uses the variable  $x_3 = \Delta \ln(1+z) = \ln[(1+z_\alpha)/(1+z_i)]$  for subset  $\alpha i$ .

#### A.3.1. $kz$ form

For functions over the  $(x_1, x_2)$  space we use a simple two-dimensional version of interpolation between values on a rectangular grid. The power-spectrum theory error  $\delta \ln P$  uses this form, as do the  $K^{gg}(k, z)$  and  $K^{\kappa\kappa}(k, z)$  nuisance functions. The only complication of note is that the nodal point  $a_{ij}$  should have a prior with variance  $\sigma_a^2 = (3/2)^2 \sigma_f^2$  if the output function is to have variance  $\sigma_f^2$ . The factor of  $(3/2)^2$  is needed to counteract the reduced variance when interpolating between grid points.

The  $kz$  nuisance function is specified by:

- the spacing  $\Delta x_1 = \Delta \ln k$  of the nodes for linearly interpolation in  $x_1$ ;

- the spacing  $\Delta x_2 = \Delta \ln(1 + z)$  of the nodes for linearly interpolation in  $x_2$ ;
- the RMS variation  $\sigma_f$  of the function allowed under the prior, which can depend on  $x_1$  and  $x_2$ .
- the fiducial dependence of  $f$  on  $x_1$  and  $x_2$ .

### A.3.2. $z\Delta z$ form

For nuisance variables over the  $(x_2, x_3)$  space ( $z$  and  $\Delta z$ ), we adopt the following strategy: we choose to have variation over  $x_3$  be described by polynomials since we usually define the range of non-catastrophic photo- $z$  errors to be bounded to some range  $|x_3| \leq \Delta_{\max}$ . We define the “ $z\Delta z$ ” functional form as follows:

$$f(x_2, x_3) = \sum_{i=0}^{N-1} a_i(x_2) P_i(\nu x_3 / \Delta_{\max}). \quad (\text{A5})$$

The Legendre coefficients are in turn defined to be linearly interpolated between a series of values  $a_{ij}$  at redshift nodes  $\{\ln(1 + z_j)\}$ . The  $a_{ij}$  become parameters of the model.

The fiducial and prior values for the  $i = 0$  terms (constant in  $x_3$ ) are treated differently than the  $i > 0$  terms. We might, for example, expect some nuisance functions to vary strongly with  $x_2$  (nominal redshift) but only slightly with  $x_3$  (photo- $z$  error) at fixed  $x_2$ .

We specify the total RMS fluctuation in  $f$  allowed by the prior to be  $\sigma_f$ . But we also specify the fraction `VarFracDZ` of the variance that is due to dependence on  $x_3$ . If we define

$$\bar{f}(x_2) \equiv \int_{-\Delta_{\max}}^{+\Delta_{\max}} dx_3 f(x_2, x_3) / 2\Delta_{\max}, \quad (\text{A6})$$

then we aim to achieve

$$\text{Var}[\bar{f}(x_2)] = \sigma_f^2 (1 - \text{VarFracDZ}) \quad (\text{A7})$$

$$\text{Var}[f(x_2, x_3) - \bar{f}(x_2)] = \sigma_f^2 (\text{VarFracDZ}). \quad (\text{A8})$$

This is achieved approximately by setting the priors on the constant terms as

$$\sigma_{0j}^2 = \frac{3}{2} \sigma_f^2 (1 - \text{VarFracDZ}) \quad (\text{A9})$$

and the  $x_3$ -dependent terms as

$$\sigma_{ij}^2 = \frac{3}{2} \sigma_f^2 (\text{VarFracDZ}) \sqrt{\frac{(2i+1)\pi\nu}{2N \sin^{-1} \nu}}. \quad (\text{A10})$$

The RMS prior variation  $\sigma_f$  can be made a function of  $x_2$  without loss of generality. We typically take fiducial values of  $a_{ij} = 0$  for  $i > 0$  in our nuisance functions, *i.e.* no fiducial dependence upon  $\Delta z$ .

To summarize, the  $z\Delta z$  nuisance function is specified by:

- the order  $N$  of the polynomial in  $x_3$ ;
- the maximum range  $\Delta_{\max}$  of applicability in the  $x_3$  axis;
- the spacing  $\Delta x_2 = \Delta \ln(1 + z)$  of the nodes for linearly interpolation in  $x_2$ ;
- the RMS variation  $\sigma_f$  of the function allowed under the prior, which can depend on  $x_2$ ;
- the fraction `VarFracDZ` of this variance that is due to  $x_3$  ( $\Delta z$ ) dependence;
- the fiducial dependence of  $f$  on  $x_2$ .

### A.3.3. $kz\Delta z$ form

The bias and correlation coefficients can, most generally, depend on scale ( $x_1$ ) as well as subset ( $x_2, x_3$ ), so we generalize to the “ $kz\Delta z$ ” functional form:

$$f(x_1, x_2, x_3) = \sum a_i(x_1, x_2) P_i(x_3). \quad (\text{A11})$$

The coefficients  $a_i$  are linearly interpolated between nodes in the two-dimensional space ( $x_1, x_2$ ). Thus the free parameters of this model become the Legendre coefficients  $a_{ijk}$ . As for the  $z\Delta z$  function, we specify the prior by the overall mean RMS variation  $\sigma_f$  (which can be a function of  $x_2$  and  $x_3$ ), plus the `VarFracDZ` specifying how much of the variance is manifested as dependence on  $\Delta z$ . The formulae for the priors  $\sigma_{ijk}$  on the nodal coefficients are derived exactly as in Equations (A9) and (A10), except that we now need factors of  $(3/2)^2$  to account for the reduced variance when interpolating in two dimensions.

The  $kz\Delta z$  function thus requires all of the specifications as the  $z\Delta z$  function, plus a spacing  $\Delta \ln k$  for nodes in the  $x_1$  axis.

## REFERENCES

- Albrecht, A., et al. 2006, Report of the Dark Energy Task Force, arXiv:astro-ph/0609591
- Amara, A., & Refregier, A. 2007, arXiv:0710.5171
- Bernstein, G. 2006, ApJ, 637, 598
- Bernstein, G. & Jain, B., 2004, ApJ, 600, 17 [BJ04]
- Bernstein, G. M., & Norberg, P. 2002, AJ, 124, 733
- Blandford, R. D., Saust, A. B., Brainerd, T. G., & Villumsen, J. V. 1991, MNRAS, 251, 600
- Bridle, S., & King, L. 2007, New Journal of Physics, 9, 444
- Cacciato, M. *et al.* (2008), arXiv:0807.4934
- Cooray, A., & Hu, W. 2001, ApJ, 554, 56
- Croft, R. A. C., & Metzler, C. A. 2000, ApJ, 545, 561
- Eisenstein, D. J., & Hu, W. 1999, ApJ, 511, 5
- Faltenbacher, A., Li, C., Mao, S., van den Bosch, F. C., Yang, X., Jing, Y. P., Pasquali, A., & Mo, H. J. 2007, ApJ, 662, L71
- Goldberg, D. M., & Bacon, D. J. 2005, ApJ, 619, 741
- Hennawi, J. F. & Spergel, D. N. 2005, ApJ, 624, 59
- Heymans, C., et al., 2006, MNRAS 368 1323
- Hirata, C. M., et al. 2004, MNRAS, 353, 529
- Hirata, C. M., & Seljak, U. 2004, Phys. Rev. D, 70, 063526
- Hirata, C. M., & Seljak, U. 2003, Phys. Rev. D, 67, 043001
- Hu, W. 1999, ApJ, 522, L21
- Hu, W., & Jain, B., 2004, Phys. Rev. D, 70, 043009
- Hu, W. & Okamoto, T. 2002, ApJ, 574, 566
- Huterer, D., Takada, M., Bernstein, G., & Jain, B. 2006, MNRAS, 366 101
- Ishak, M., Hirata, C. M., McDonald, P., & Seljak, U. 2004, Phys. Rev. D, 69, 083514
- Jain, B. 2002, ApJ, 580, L3

- Jain, B., & Seljak, U. 1997, ApJ, 484, 560
- Jain, B., & Taylor, A. 2003, Phys. Rev. Lett., 91, 141302
- Jain, B., Connolly, A., & Takada, M. 2007, Journal of Cosmology and Astro-Particle Physics, 3, 13
- Jing, Y. P., Zhang, P., Lin, W. P., Gao, L., & Springel, V. 2006, ApJ, 640, L119
- Kaiser, N. 1992, ApJ, 388, 272
- King, L. J., & Schneider, P. 2003, A&A, 398, 23
- Knox, L., Song, Y.-S., & Tyson, J. A. 2006, Phys. Rev. D, 74, 023512
- Komatsu, E., et al. 2008, arXiv:0803.0547
- Lee, J. & Pen, U.-L. 2008, arXiv:0807.1538
- Ma, Z., & Bernstein, G. 2008, ApJ, 682, 39
- Ma, Z., Hu, W., & Huterer, D. 2006, ApJ, 636, 21
- Mandelbaum, R., Hirata, C. M., Ishak, M., Seljak, U., & Brinkmann, J. 2006, MNRAS, 367, 611
- Marian, L., & Bernstein, G. M. 2006, Phys. Rev. D, 73, 123525
- Metcalf, R. B., & White, S. D. M. 2007, MNRAS, 381, 447
- Miralda-Escudé, J. 1991, ApJ, 380, 1
- Newman, J. A. 2008, arXiv:0805.1409
- Pen, U.-L. 2004, New Astronomy, 9, 417
- Schneider, M., Knox, L., Zhan, H., & Connolly, A. 2006, ApJ, 651, 14
- Smith, R. E., *et al.*, 2003, MNRAS, 341, 1311
- Song, Y.-S. & Knox, L. 2004,
- Takada, M., & Jain, B. 2004, MNRAS, 348, 897
- Tegmark, M., Taylor, A., Heavens, A., 1997, ApJ, 480, 22
- S. Wang, J. Khoury, Z. Haiman et al. 2004, Phys. Rev. D, 70, 123008
- Zahn, O., & Zaldarriaga, M. 2006, ApJ, 653, 922
- Zhan, H. 2006, Journal of Cosmology and Astro-Particle Physics, 8, 8
- Zhan, H., & Knox, L. 2004, ApJ, 616, L75

Zhang, J., Hui, L., & Stebbins, A. 2003, astro-ph/0312348